# A New Technique for Gas-phase Kinetic Spectroscopy of Molecules in the Triplet State

**Abstract:** A recently developed experimental method is described to populate by Hg photosensitization and observe by absorption spectroscopy the triplet states of polyatomic molecules in the gas phase; detailed discussion and analysis of the experiment are given. The technique can be used to investigate triplet states that cannot be populated efficiently by the intersystem crossing process and to detect triplet absorption bands located within the wavelength range of ground-state absorption of a molecule. A modulation scheme, based on a novel type of Hg resonance light source—an rf-driven toroid capable of modulation frequencies up to 250 kHz—is used for monitoring the optical absorption (by phase-sensitive detection) and measuring the lifetime of the transient species. Sensitivity is comparable with that of flash spectroscopy for transients that decay by a second-order process. Results obtained for several aromatic hydrocarbons are reviewed. New transitions were detected by this method for triplet-state naphthalene, and the absorption spectra and decay kinetics of triplet-state benzene and toluene were measured for the first time. Some applications of the technique to problems other than triplet-state spectroscopy are illustrated or outlined.

#### **Contents**

Introduction

Description and analysis of experiment

- · General outline
- Sensitivity and comparison with flash spectroscopy
- Modulation response of first- and second-order reactions

# Apparatus

- Optical train
- Optimization of absorption cell
- Construction of mercury lamp, absorption cell and auxiliary systems
- · Properties of modulated mercury arc
- Phase measurements
- · Elimination of stray light
- Separation of absorption and emission signals by double modulation
- Spurious absorption signals
- Direct recording of absorption

# Results

- First-order decay kinetics
- Triplet-state absorption spectra
- Second-order decay kinetics

# Outlook

# 10 Appendix

#### Introduction

In this paper we present a detailed discussion of the design, construction and operation of a recently developed experimental technique for the spectroscopic detection in the gas phase of molecules in their lowest electronic triplet states. Preliminary results obtained with this technique have been described briefly [1–3].

It is characteristic of previous methods serving this purpose that they rely on the intersystem crossing process (see Fig. 1) for populating the metastable state [4, 5]. Consequently, compounds that exhibit efficient intersystem crossing are the only ones that have been studied. These include the aromatic and heteroaromatic compounds and some ketones. However, it is well known that the existence of a low-lying, metastable triplet state is a fairly general property among molecules. The triplet states of olefins, acetylenes, CO2 and other compounds have been invoked as intermediates in photochemical reactions, but these intermediates have never been directly observed. Their chemical reactivities, unimolecular lifetimes and exact energies are largely unknown. The principal reason for this situation is the lack of a direct and efficient process for populating these states, which would make them amenable to spectroscopic investigation.

When the process of intersystem crossing is used to populate the triplet state of a compound, efficient excitation occurs only if the sample absorbs a significant portion of the exciting light. Thus the wavelength range of the ground state absorption of the sample is partly opaque, and experience has shown that this opacity makes it difficult or impossible to detect transient triplet optical absorption bands in this region. Cases in point are benzene and naphthalene, which are discussed in later sections of this paper.

The technique we describe was developed for the purpose of overcoming, in suitable cases, the difficulties outlined above. It has been successfully applied to the detection of triplet absorption bands that are located within the region of ground-state absorption and could not be observed by previous methods. A noteworthy aspect of this technique is that it provides the absorption spectra of triplet states in the gas phase. Gas-phase observations are currently available for only a few molecules. Most of the known triplet spectra were obtained in the liquid and solid phases, for reasons of experimental feasibility. However, comparison of data obtained in a condensed phase with theoretical calculations for the free molecule or with electron scattering results is hampered by the fact that the spectroscopically observed excited states undergo relatively strong interactions with the surrounding medium. Such interaction not only results in spectral shifts, broadening and distortion, but can also cause the disappearance in the condensed phase of entire band systems, as in the case of napthalene [6, 7].

Looking to photochemical methods for alternatives to the intersystem crossing process for populating the triplet state, one finds that energy transfer schemes have long been used to initiate triplet reactions. The most important technique of this type for gas-phase work is Hg photosensitization, in which the  $6^3P_1$  (4.89-eV) and  $6^3P_0$  (4.67-eV) excited states of the Hg atom are used as energy donors. The former state is excited when Hg atoms absorb 253.7-nm resonance radiation:

$$Hg(^{1}S_{0}) + h\nu(253.7 \text{ nm}) \rightarrow Hg(^{3}P_{1}).$$
 (1)

The latter, metastable state can be populated by collisions of the  ${}^{3}P_{1}$  state with  $N_{2}$  and a number of other molecules [8] according to the reaction

$$Hg(^{3}P_{1}) + N_{2}(v = 0) \rightarrow Hg(^{3}P_{0}) + N_{2}(v = 1).$$
 (2)

Excellent reviews of the subject of Hg-photosensitized reactions exist [9–11]. The observed products and kinetic properties of these reactions have led to the postulate [12] that the most probable primary process is

$$Hg(^{3}P_{1}, ^{3}P_{0}) + M(S_{0}) \rightarrow M(T_{1}) + Hg(^{1}S_{0}),$$
 (3)

if the acceptor molecule M has a triplet state  $T_1$  lower in energy than the excited state of the Hg atom.

This alternative path for populating the triplet state, indicated in the right-hand part of Fig. 1, has not been used in the past for purposes of triplet-state spectroscopy. The stationary concentration of triplet molecules in a

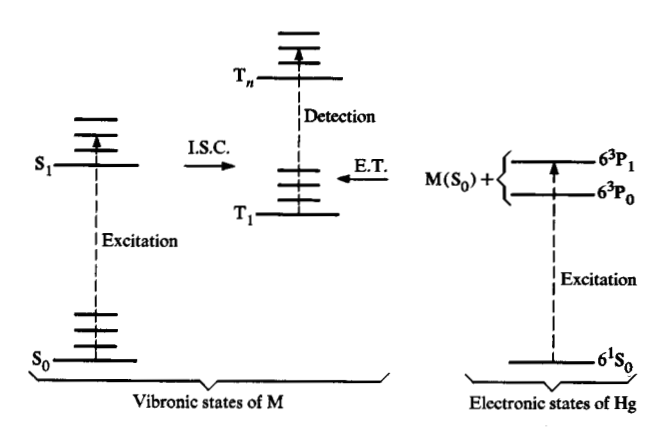


Figure 1 Excitation of triplet states by intersystem crossing (I. S. C.) and energy transfer (E. T.);  $S_0$  and  $S_1$  are singlet electronic states of the molecule M and are connected by an optically allowed transition;  $T_1$  and  $T_n$  are triplet states of M, also connected by an optical transition, which serves for detection of state  $T_1$ .

conventional Hg-photosensitization experiment is too low to be detected by standard photometric techniques. Also, the technique of flash spectroscopy [13] has not been readily applicable, because of the low efficiency of the available flash light-sources in producing excited Hg atoms. This difficulty has been partly overcome by the recent development of a monochromatic 253.7-nm flash light-source by Callear and coworkers [14, 15]. Although it is more efficient for exciting Hg atoms, the intensity of this light source is more than three orders of magnitude lower than that of a Xe flash lamp.

In our approach a modulated source of 253.7-nm radiation is used for the generation of transients in Hg-photosensitized reactions. As is described in a later section, the modulation approach has a considerable advantage in sensitivity. Some preliminary results obtained with this method have been reported [1–3]. The purpose of the present paper is to give a detailed description of the experimental technique, to demonstrate its usefulness by summarizing the observations made with it so far, and to indicate some of the possible future applications.

# Description and analysis of experiment

# General outline

Since the brightness of a low-pressure Hg-discharge source (principal light output at 253.7 nm [16]) is relatively low, a large source area and an arrangement providing for efficient transfer of radiation to the reaction volume are necessary to achieve sufficient excitation density. For this purpose we use a concentric arrangement, as in prelaser Raman spectroscopy.

The experiment is outlined in Fig. 2. Vapor of compound M to be investigated is mixed with Hg vapor and an inert

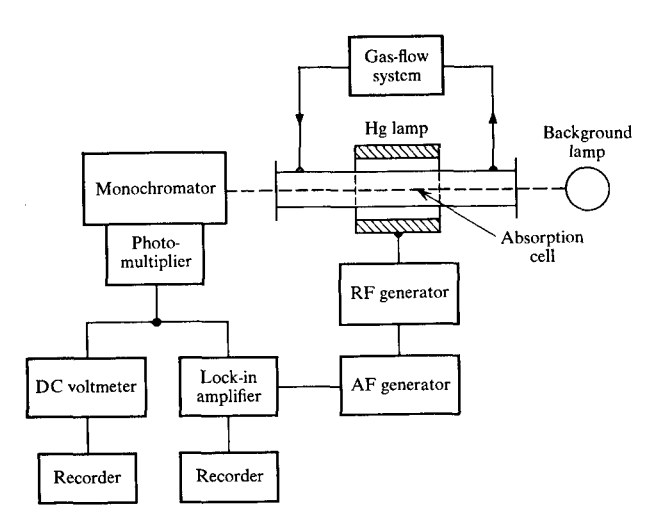
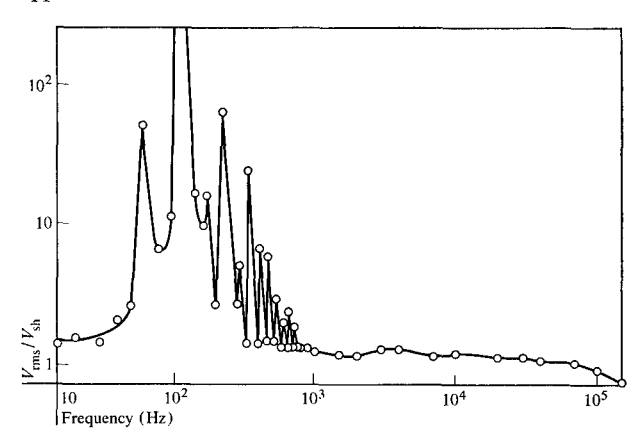


Figure 2 Experimental system for gas-phase kinetic spectroscopy.

Figure 3 Frequency spectrum of Xe arc fluctuations. The source was a Hanovia Model 901 C-1 150-W high-pressure Xe lamp. Its emission at 300 nm was analyzed with a frequency bandwidth of 12.5 Hz. In a log-log plot, the ratio of the observed ac signal  $V_{\rm rms}$  to the calculated shotnoise voltage  $V_{\rm sh}$  is shown as a function of the center frequency of the measurement. Low frequency peaks are produced by an incompletely filtered power supply. At the high frequency end, instrument characteristics cause an apparent falloff below shot-noise level.



carrier gas, e.g., N<sub>2</sub>, and flows through a cylindrical, multiple-path absorption cell. The cell is enclosed by a toroidal, low-pressure Hg lamp modulated over a wide frequency range by driving the lamp with an rf generator, whose amplitude is modulated by an audio oscillator. Modulation frequencies up to about 250 kHz can be used. Through the series of reactions (1), (2) and (3), the incident radiation produces a modulated concentration of excited molecules in the cell. Absorption by these transient

molecules is detected by passing a beam of white light from a background source through the cell and a monochromator, and by monitoring the modulation of the transmitted light as a function of wavelength with a lock-in amplifier. A simultaneous measurement of the dc photocurrent allows the reduction of this signal to an rms absorption value. Emission is detected in a similar way. The lifetime of an absorbing or emitting transient species is determined from the phase shift of its signal with respect to the 253.7-nm emission of the Hg lamp.

# • Sensitivity and comparison with flash spectroscopy

Our technique makes possible a direct and continuous photometric recording of transient spectra and phase shifts, which is not possible with the flash spectroscopic technique [13]. When measuring absorption of a transient species, we can usually eliminate unwanted signals from fluorescence of the compound under investigation, or from absorption by reaction products, by synchronizing the detector so that it is out of phase with the unwanted signal. These two advantages can be fully realized only if a wide range of modulation frequencies is available. Most other approaches to modulated absorption spectroscopy operate only at low modulation frequencies [17–22].

The sensitivity of pulse methods for photometric detection of transient absorption spectra is limited by the shot noise of the background source. This is also true for the modulation approach if the noise spectrum of the source reaches the shot-noise level well within the range of available modulation frequencies. That the noise spectrum does reach the shot-noise level in this range is shown in Fig. 3, which represents the noise spectrum of a commonly used background source. The detection bandwidth for a flash-excited experiment is at least 10<sup>6</sup> Hz, but in a modulation experiment the bandwidth is typically 1 to  $10^{-2}$  Hz. The resulting reduction in rms noise voltage is a factor of  $10^3$  to  $10^4$  [23]. This reduction is borne out by the weakest absorption that can be detected in practice, about  $10^{-2}$  for a flash-excited experiment and  $10^{-5}$  to 10<sup>-6</sup> for our modulation method.

Pumping intensities (I) and relative sensitivities for an average reaction volume are listed in Table 1 for both pulse and modulation methods. When the transient molecule lifetime is short compared to the pulse duration, the stationary transient concentration is  $I/k_1$  for a first-order decay with rate constant  $k_1$ , and  $(I/k_2)^{\frac{1}{2}}$  for a second-order decay with rate constant  $k_2$ . It follows that the Xe flash technique is best for photometric detection of first-order transients, while for second-order transients the modulated Hg arc technique is best. If the transient lifetime is longer than the pulse duration, the stationary concentration will not be attained in the pulse experiment and the comparison will be more favorable for the modulation technique.

• Modulation response of first- and second-order reactions Since the Hg arc is sinusoidally modulated, the rate of 253.7-nm light absorption per unit volume can be described by

$$I = I_0 + I_1 \exp(i\omega t), \tag{4}$$

where  $\omega$  is the angular frequency of modulation and the imaginary part of Eq. (4) is used for convenience in the case of linear responses, e.g., first-order reactions. Under conditions of total quenching, as represented by the sequence of reactions (1) through (3), I (expressed in Einstein-l<sup>-1</sup>-sec<sup>-1</sup>) is also the rate of formation of transient molecules per unit volume.

For later reference we recall two simple results for modulated first-order reactions, the first of which is often used in the context of phase fluorometry [24]. For concentration c of a species S formed at rate I and decaying by a first-order reaction with rate constant  $k_1$ , the periodic solution of the rate equation is

$$c = I_0/k_1 + [I_1/(k_1^2 + \omega^2)^{\frac{1}{2}}] \exp [i(\omega t + \phi_1)],$$
  

$$\tan \phi_1 = -\omega/k_1.$$
 (5)

If species S decays to species S' with rate constant  $k_1$ , and S' decays with rate constant  $k_1$ ', one has for the concentration c' of S',

$$c' = I_0/k_1' + [k_1I_1/(k_1^2 + \omega^2)^{\frac{1}{2}}(k_1' + \omega^2)^{\frac{1}{2}}]$$

$$\times \exp[i(\omega t + \phi_1 + \phi_2)], \quad \tan \phi_2 = -\omega/k_1'. \tag{6}$$

This result can be generalized to a sequence of first-order reactions of any length; the phase shifts of the individual steps are additive. Reactions (2) and (3) are an example of a sequence of two (pseudo) first-order reactions. In the case of the aromatic hydrocarbon triplet states discussed below, conditions can often be chosen such that the phase shifts introduced by steps (2) and (3) are negligible compared to the shift due to the decay of  $M(T_1)$ .

Equation (6) is of interest because it shows that if S' is a stable product, and therefore  $k_1' \ll \omega$  and  $\phi_2 \approx -90^\circ$ , the lifetime of the intermediate species S can be determined by measuring the phase shift of product S'.

If a transient decays by both first- and second-order reactions, the rate equation for its concentration c is

$$dc/dt = I - k_1 c - k_2 c^2, (7)$$

with I given by the real part of Eq. (4). Equation (7) is a general Riccati equation whose solution cannot be obtained in closed form [25]. A solution for the limit of high modulation frequency can be derived by observing that c will be almost constant and equal to

$$\bar{c} = [-k_1 + (k_1^2 + 4I_0k_2)^{\frac{1}{2}}]/2k_2,$$
 (8)

Table 1 Comparison of intensities and signal-to-noise ratios relative to the modulated Hg arc for photometric detection of transient absorption in pulse and modulation experiments,

Intensity (Einstein/sec)	Relative intensity	Relative S/N	
		First- order decay	Second- order decay
6.6	$3 \times 10^{5}$	300	0.6
0.6	$3 \times 10^4$	30	0.2
$2.1 \times 10^{-3}$	102	0.1	0.01
$2.1 \times 10^{-5}$	1	1	1
	$\frac{(Einstein/sec)}{6.6}$ $0.6$ $2.1 \times 10^{-3}$	(Einstein/sec) intensity  6.6 3 $\times$ 10 <sup>5</sup> 0.6 3 $\times$ 10 <sup>4</sup> 2.1 $\times$ 10 <sup>-3</sup> 10 <sup>2</sup>	Intensity (Einstein/sec) Relative intensity decay $6.6  3 \times 10^{5}  300 \\ 0.6  3 \times 10^{4}  30$ $2.1 \times 10^{-3}  10^{2}  0.1$

Detection bandwidth of 106 Hz assumed.

which is the stationary solution for  $I = I_0$ . Writing  $c(t) = \bar{c} + \Delta c(t)$  and retaining only terms linear in  $\Delta c$ , one can obtain a solution of Eq. (7) in the form of Eq. (5):

$$c(t) = \bar{c} + [I_1/(k^2 + \omega^2)^{\frac{1}{2}}] \exp[i(\omega t + \phi)],$$
 (9)

where the modulated part is now governed by an apparentfirst-order rate constant

$$k = 2k_2\bar{c} + k_1 = (k_1^2 + 4k_2I_0)^{\frac{1}{2}}. (10)$$

This solution can be shown to be quite good even at lower frequencies for which the variations of c in time are relatively large. The exact periodic solution of Eq. (7) was calculated numerically over a wide range of parameters by iterated Runge-Kutta integration. The amplitude and phase shift of the fundamental component—the principal quantities of interest in an experiment-were then obtained by numerical Fourier analysis; some of their values for the case  $I_1 = I_0$ ,  $k_1 = 0$  are given in Table 2 for both the exact and the approximate first-order-type solutions. The latter solution deviates by about ten percent in tan  $\phi$ and five percent in the amplitude at a phase shift of 29° (tan  $\phi = 0.554$ ), but the deviation decreases rapidly with increasing phase shift. If  $I_1 < I_0$  or  $k_1 > 0$ , the agreement is even better.

Thus at sufficiently large phase shifts Eq. (9) in conjunction with Eq. (10) can be used to evaluate the rate constants of a combined first- and second-order decay process. A plot of  $k^2$ , as determined from phase measurements, vs  $I_0$  should be a straight line whose slope and intercept determine  $k_2$  and  $k_1$ , respectively.

b G. Porter, in *Techniques of Organic Chemistry*, edited by S. L. Friess, E. S. Lewis and A. Weissberger, 2nd Ed., Vol. III, Part II, Interscience Publishers, Inc., New York 1961, Chap. XIX.

A. B. Callear and R. E. M. Hedges, *Nature* 218, 163 (1968).

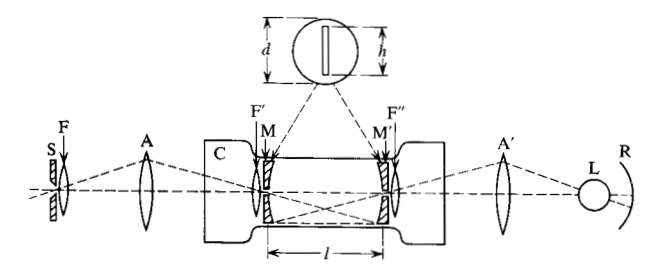
d Detection bandwidth of 1 Hz assumed.

**Table 2** Comparison of solutions of the nonlinear rate equation (7) for a case of second-order decay  $(k_1 = 0)$  with  $I_1 = I_0$ .

Solution	Frequency parameter $\omega(k_2I_0)^{-\frac{1}{2}}$	Phase shift <sup>a</sup> tan ф	$Amplitude \ parameter^a \ c(k_2/I_0)^{1\over 2}$
Exact	1.000	0.554	0.471
	1.585	0.841	0.402
	2.512	1.295	0.314
First-order	1.000	0.500	0.447
[Eqs. (9) and (10)]	1.585	0.793	0.392
	2.512	1.256	0.311

a For the fundamental frequency.

Figure 4 Optical train used with the Pfund cell: S, monochromator entrance slit; F, F' and F", field lenses; A and A', imaging lenses; M and M', spherical mirrors of diameter d and radius of curvature 2l, with slits of height h; C, absorption cell; L, background light source; and R, spherical reflector.



Besides the transient concentrations discussed so far, there are other effects that can lead to a modulation of background light transmitted through the reaction cell. It is shown in the Appendix that effects due to periodic heating can usually be kept small. Spurious signals due to the apparatus are discussed in another section.

# **Apparatus**

# • Optical train

A multiple-path arrangement due to Pfund [26] was preferred to the more frequently used White multiple-path cell [27]. The Pfund cell consists of two slotted spherical mirrors separated by their focal length *l*. The slit of the monochromator is imaged by a lens onto the slot in one mirror. From there the rays traverse the cell three times and exit through the slot in the second mirror, which is in turn imaged onto the light source. The optical train is shown in Fig. 4.

## • Optimization of absorption cell

For a given monochromator with aperture  $f_0$  and slit height  $h_0$ , there is an optimal design of the absorption cell if either its length l or its diameter d is specified. The quantity to be optimized is the signal-to-noise ratio S/N for measuring the absorption A of a transient. If the intensity of the background source reaching the detector is P, the ratio is

$$S/N \propto AP/P^{\frac{1}{2}} = AP^{\frac{1}{2}},$$
 (11)

since the major source of noise is shot noise.

The amount of light reaching the cell from the surrounding Hg-vapor discharge is proportional to the surface area of the cell; hence the average power absorbed per unit volume varies as  $d^{-1}$ . Thus, for a transient decaying by a first-order process,  $A \propto l d^{-1}$ , and in the case of a second-order decay,  $A \propto l d^{-\frac{1}{2}}$ .

If the monochromator aperture is properly matched by a lens to the cell aperture f = l/d, the main geometry-dependent intensity loss is due to vignetting, which for a Pfund cell can be approximated [28] by

$$P = P_0(1 - h/\pi d) = P_0(1 - lh_0/\pi d^2 f_0), \tag{12}$$

with  $h = h_0 f/f_0$ . Thus, for a first-order transient,

$$S/N \propto l d^{-1} (1 - lh_0/\pi d^2 f_0)^{\frac{1}{2}}.$$
 (13)

From Eq. (13) one can derive that, for a given l, the optimal values are

$$d_{\text{opt}} = (2lh_0/\pi f_0)^{\frac{1}{2}} \text{ and } h_{\text{opt}} = h_0 l/f_0 d_{\text{opt}}$$
 (14)

for a first-order transient. For a signal from a species decaying by a second-order process, one finds in the same way

$$d_{\text{opt}} = (3lh_0/\pi f_0)^{\frac{1}{2}}. (15)$$

Optimal values of l for a given value of d can be derived in a similar manner. There are, of course, no simultaneous optima for l and d, since S/N can always be improved by making the cell larger. By substituting Eq. (14) or (15) into (13), one finds this improvement to be proportional to  $l^{\frac{1}{2}}$ , i.e., the sensitivity of the apparatus varies roughly as the square root of its size.

If, in order to minimize aperture and reflection losses, the multiple-path mirrors are mounted inside the photochemical reactor, their uv reflectivity  $\rho$  will in general be considerably below 1.0. This condition tends to cancel the advantages of the White cell [27], which has no vignetting loss and provides longer absorption paths. The optimal number of passes, for absorption measurements limited by shot noise, is  $-2/\ln \rho$ , rounded to the next multiple of four. Also, since the White arrangement has two apertures side by side, it requires a cell diameter about twice that of the Pfund cell for the same length, thus lowering the transient concentration accordingly. Hence one finds that for  $\rho < 0.8$ , the Pfund cell is to be preferred. The main advantage of the Pfund cell is that it is less sensitive to reflection losses caused by reaction product deposits on the multiple-path mirrors.

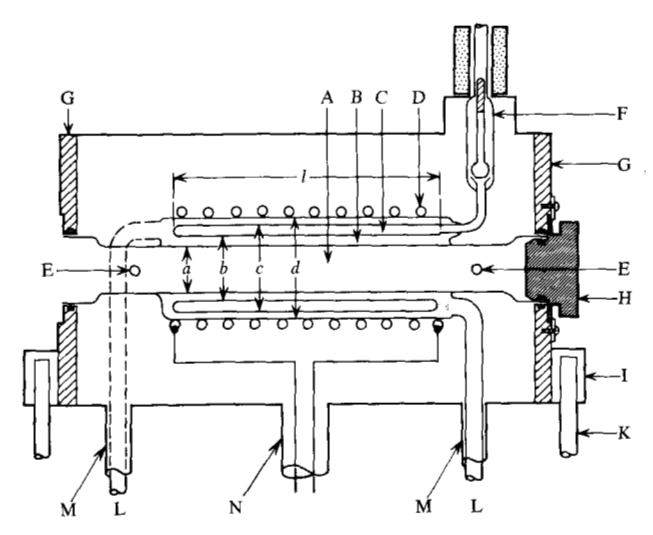


Figure 5 Hg lamp and absorption cell assembly: A, absorption cell; B, lamp-cooling mantle; C, lamp toroid; D, rf driving coil; E, entrance and exit ports of flow system; F, magnetically operated ball-joint valve; G, mounting plates (connected by four metal bars not shown); H, cell insert holding optical components and cell window (detail in Fig. 6); I, insulator block; K, bench mounting rod; L, coolant hoses; M, hose shields; N, rf conductor tunnel to matchbox circuit. Dimensions (in cm): l = 20; outside diameters a = 3.5, b = 4.8, c = 6.4 and d = 7.4.

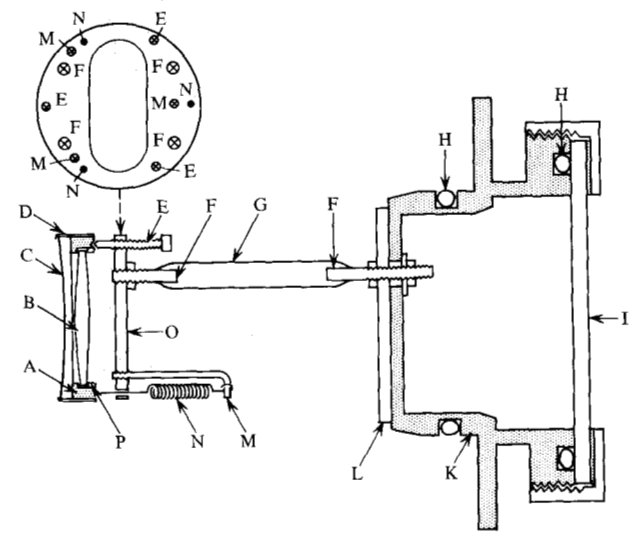


Figure 6 Absorption cell insert: A, lens- and mirror-mounting ring; B, field lens; C, mirror (3.0-cm diameter); D, mirror clamp; E, mirror alignment screw; F, Kovar rod; G, glass rod; H, O rings; I, quartz window (6.35-cm diameter); K, stainless steel body; L, table base; M, spring support; O, table top; P, expansion ring. Holes in K, L and O for light passage and mirror alignment are omitted from the longitudinal section. The arrangement of parts E, F and N around the axis is shown in the front view of part O.

# • Construction of Hg lamp, absorption cell and auxiliary systems

An electrodeless, rf-excited, Hg arc is used because light sources of this type emit particularly intense and narrow resonance lines [29], and rf amplitude-modulation provides a means for modulating the light output in a wide frequency band. Toroidal rf-driven arcs have been used previously as sources for the visible Hg and Cd lines in Raman spectroscopy [30].

Figure 5 is a longitudinal section through the Hg lamp and absorption cell assembly, including the external connections and housing, but with the optical components removed. It was made from four concentric quartz tubes. The lamp toroid is held in place by notches in the outermost tube. It is connected through a magnetically operated ball-joint valve to a separate, grease-free, high-vacuum system, used to fill the lamp with pure Ar to a pressure of a few Torr. During operation of the lamp the volume above the valve is evacuated.

The lamp toroid is completely embedded in cooling water, which is circulated at a rate of 16 l/min through the lamp enclosure. Connecting hoses are shielded to prevent rf pickup by the photometric system.

The absorption cell has entrance and exit ports for reactant gas flow and straight open ends that are closed off by separate inserts which hold the optical components and windows. One of these inserts is shown in detail in Fig. 6. The mirror and lens are electrically insulated from the main body of the insert. They form the top of a table with four glass-rod legs, which can be shifted laterally with respect to the main body and centered independently in the narrow part of the absorption cell. Figure 7 is a picture of the complete lamp and multiple-path assembly.

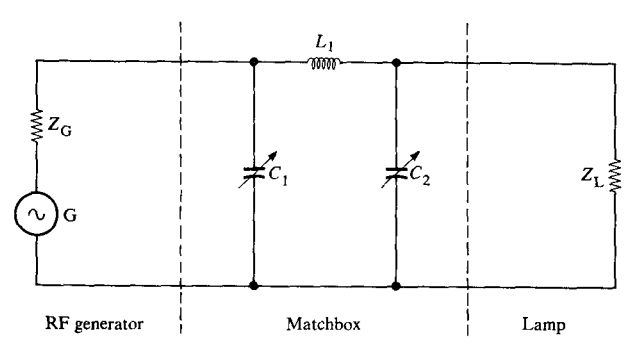
The Hg lamp is driven inductively by a surrounding nineturn primary coil of 0.25-in. copper tubing that fits over the outermost quartz tube. The lamp impedance is matched to the 50-ohm impedance of the generator through an intermediate  $\pi$ -network or "matchbox," as shown in Fig. 8. A 6-kW, 13.5-MHz rf generator, designed for cathode sputtering, was adapted for this experiment [31]. Low-level amplitude modulation was introduced in the exciter section of the generator [32]. Careful rf shielding and grounding are necessary to prevent interference of rf pickup with photometric measurements.

A proportionally controlled heat exchanger is used to keep the cooling water at a constant temperature. Since the phase of the 253.7-nm emission relative to the modulating oscillator varies with lamp temperature, it is necessary to control the temperature of the water flowing to the lamp within 0.1°C to make these phase variations negligibly small. The normal lamp operating temperature is 40°C. Optical transmission-filter substances can be added to



Figure 7 Hg lamp and absorption cell assembly. The background light beam from a high-pressure Xe lamp enters the cell from the right; it is made visible by filling the absorption cell with smoke.

Figure 8 Lamp-impedance matching network: G, rf generator (13.5 MHz, 6 kW max);  $Z_6$ , 50 ohms (generator output impedance);  $L_1$ ,  $0.4 \times 10^{-6}$ H (two-turn coil, 3.5-in. diameter, 1.5-in. length);  $C_1$ , 0 to 2000 pF (Jennings UCSFX 2000 7.5 S);  $C_2$ , 0 to 1200 pF (Jennings UCSFX 1200 7.5 S);  $Z_L$ , lamp impedance (see text).



the cooling water. Their use is limited to water-soluble materials that do not greatly increase the electrical conductivity of the coolant. A cyanine-like dye [33] for stray-light rejection in the 280- to 340-nm range was used in this way. Also, a very convenient neutral-density filter was found in the form of an aqueous solution of colloidal graphite, stabilized by addition of NH<sub>3</sub>.

The gas flow system is designed in such a way that pure carrier gas and carrier gas saturated with reactants at controlled temperatures can be mixed in any proportion before entering the absorption cell. Provision for adding flow from a gas mixture storage system is also included. The carrier gas flows are metered in the upstream section at constant pressure, while reactants are picked up in

the middle section at the cell pressure, which is regulated by a Cartesian-diver type manostat. Traps at the entrance and exit of the flow system eliminate condensible impurities and collect reaction products, respectively.

Other parts of the experimental system are based on standard techniques: A Bausch and Lomb 50-cm grating monochromator with a 1200-line/mm grating blazed at 300 nm is used, with an Amperex 150 UVP photomultiplier attached to it. The ac part of the signal is measured across a 3-kohm load resistor by a Princeton Applied Research lock-in amplifier model HR8, fitted with a type C preamplifier. The dc part of the signal is amplified by a high-input-impedance operational amplifier incorporated into the photomultiplier housing, and then recorded separately. Through a viewing port equipped with a 253.7-nm bandpass filter [33], the output of the Hg lamp is continuously monitored by an RCA 1P28 photomultiplier and displayed on an oscilloscope.

# • Properties of modulated Hg arc

Depending on the rf power level, the lamp operates either in the glow discharge or the arc mode. At sufficiently high input power (500 to 1000 W) the arc mode consists of a uniform and steady ring discharge extending throughout the toroid. Optimum matching conditions differ for the two modes, since they correspond to widely different specific resistances of the discharge. Impurities in the lamp filling strongly affect the power required for the mode transition, and thus the modulation behavior of the lamp.

The electrical characteristics of the lamp in the arc regime are those of a non-ideally coupled rf transformer. The input impedance  $Z_L$  of such a circuit, with its secondary side loaded by a resistance R, can be shown [34] to be

$$Z_{\rm L} = i\omega L_1(R + \sigma i\omega L_2)/(R + i\omega L_2), \qquad (16)$$

if stray capacitances can be neglected. In Eq. (16)  $L_1$  and  $L_2$  are the primary and secondary inductances,  $\omega$  is the angular radio frequency and  $1 - \sigma$  is the degree of coupling.

Measurements were made on a toroidal lamp (without cooling mantle) with dimensions similar to those indicated in Fig. 5, but excited by a 12-turn primary coil. The value of R was estimated from the toroid dimensions, using a specific resistance of 0.6 ohm-cm for the arc discharge, which was estimated from data given by Lossing et al. [35]; the value of  $L_2$  was obtained by treating the discharge as a single-turn coil [36]. Taking  $\sigma = 0.15$  and writing  $Z_L = R' + i\omega L'$ , both the calculated [Eq. (16)] and observed values were R' = 140 ohms and  $L' = 1.9 \times 10^{-6}$  H.

The modulation response of the 253.7-nm light output is shown in Fig. 9. Full modulation is possible up to 100 kHz, and a useful response is still present at 250 kHz. Above 1 kHz nearly harmonic, full modulation can be obtained. For example, a second-harmonic content of

four percent was measured at 2 kHz with full modulation. Below 1 kHz distortion occurs if full modulation is attempted. This is probably due to alternation between the glow-discharge and the arc modes, as indicated by poor rf matching. Full modulation of square-wave type, however, can easily be accomplished in this frequency region.

The response-limiting mechanism in the lamp is trapping of the 253.7-nm resonance radiation by Hg vapor. Trapping is indicated by an increasing phase lag of the 253.7-nm emission relative to other nonresonant Hg lines with increasing modulation frequency. However, the response is considerably better than would be expected from a uniformly excited slab of Hg vapor, saturated at 40°C, with a thickness equal to that of the toroid. The response of the slab is indicated in Fig. 9, curve (c), which corresponds to a limiting decay time of  $1.8 \times 10^{-6}$  sec, calculated from Milne's theory using an average of Samson's and Kenty's equivalent opacities [37]. The reason for the shorter decay time of the lamp may be a higher density of emitting Hg atoms near the toroid walls, as would be produced by the skin effect. This effect is expected to disappear at low Ar pressures, in which case the electron mean-free-path becomes comparable to the toroid thickness. Indeed, a poorer modulation response is observed as the Ar pressure in the lamp is lowered. Lower pressure also results in a greater light intensity and a less stable discharge. Pressure broadening of the resonance line at an Ar pressure of 5 Torr is insignificant and does not offer an explanation for the enhanced modulation response [38].

The power density of 253.7-nm Hg radiation absorbed by Hg vapor in the cell was determined by using the Hg-photosensitized decomposition of ethylene [39] and cis-trans isomerization of butene-2 [40] as actinometers. The lamp shown in Fig. 5, with the cooling fluid at 40°C, filled with Ar to a pressure of 5 Torr and driven with 800 W of rf power, supplied  $5.6 \pm 0.6$  W-m<sup>-3</sup> when the pressure of Hg vapor in the absorption cell was 0.3 mTorr. With baffles for elimination of stray light inserted in the absorption cell, the power density was 2.5 W-m<sup>-3</sup>. This value increased to 3.8 W-m<sup>-3</sup> on increasing the Hg pressure to 0.9 mTorr, which indicated incomplete absorption and thus fairly homogeneous excitation at the lower Hg pressure. Power density increased more than threefold when the Ar pressure was reduced to 0.3 Torr.

Lamp preparation is of critical importance and determines the behavior of the modulated arc. New lamps have to be thoroughly cleaned by running a vigorous Hg discharge while at the same time continuously pumping away evolving impurities. A lamp conditioned in this manner can be run for an hour or longer without significant deterioration. After extended use a brown deposit builds up inside the toroid which can be cleaned out with a mixture of H<sub>2</sub>O, HF and HNO<sub>3</sub>.

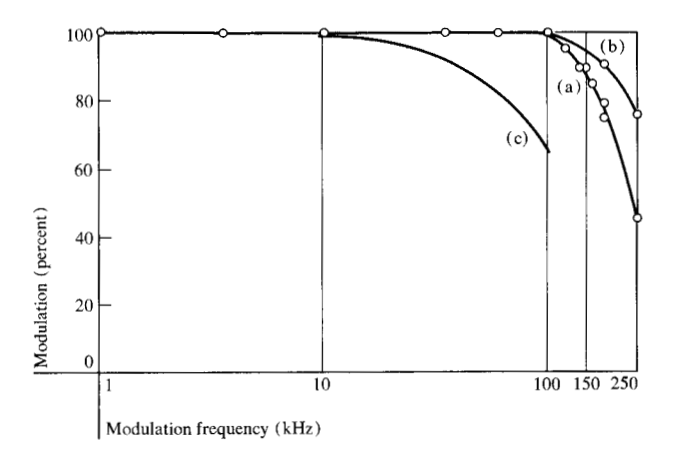


Figure 9 Modulation response of the rf-excited Hg arc emission at 253.7 nm (lamp temperature, 40°C; filling, 5 Torr Ar): (a) Observed response; (b) observed response corrected for incomplete rf modulation above 100 kHz (correction obtained by extrapolating the observed relation between rf and light modulation); and (c) calculated modulation response of 0.6-cm slab of Hg vapor saturated at 40°C.

#### Phase measurements

Phase angles are measured by a substitution method. First the monochromator is set at the wavelength of a reference emission or absorption and this signal is zeroed with the phase control of the lock-in-amplifier reference channel. Then the monochromator is reset at, or scanned over, the emission or absorption feature of interest and the in-phase and out-of-phase components,  $s_i$  and  $s_o$ , are recorded using a 90° phase-shift switch. By applying different sensitivities for determining  $s_i$  and  $s_o$ , even small phase angles can be detected with good accuracy. Tests with a calibrated RC circuit at 60, 100 and 150 kHz showed that small angles could be measured accurately within 0.1°.

Reference signals representative of the phase of 253.7-nm radiation incident on the cell are 1) stray light at this wavelength, if radiation diffusion in the cell is suppressed by high quencher concentration or complete absence of Hg vapor, and 2) short-lived molecular fluorescence excited by this wavelength, if no delayed fluorescence component is present. For transients generated from  $Hg(^{3}P_{0})$ atoms, absorption by these atoms is also a suitable reference; it can be detected with high sensitivity using the 296.7- and 404.7-nm lines of a low pressure Hg background light source. The 253.7-nm emission external to the lamp toroid lags in phase relative to the inside emission at high modulation frequencies and is therefore not a good reference signal for light-induced processes in the absorption cell. No phase differences of this type were noted for nonresonant Hg lines.

The thermostatically controlled Hg arc has good phase stability; i.e., drift and random variations of the phase of the 253.7-nm emission relative to the modulating oscil-

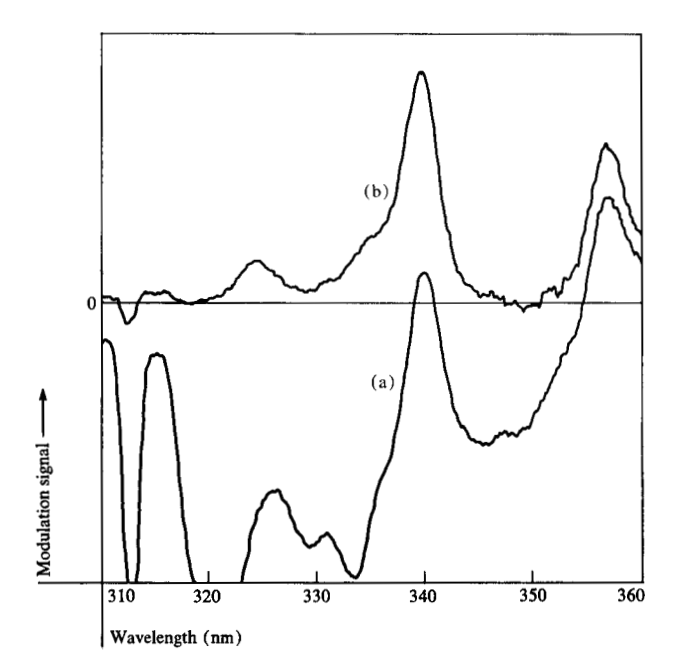


Figure 10 Effect of double modulation: (a) Modulation signal with naphthalene vapor (in  $N_2$ , in presence of Hg) observed in phase with the exciting 253.7-nm radiation. The trace is a superposition of triplet absorption and fluorescence emission with opposite signs. (b) The same signal detected by double modulation. Fluorescence is completely rejected. Modulation frequencies were 1 kHz for the exciting light and 5 Hz for the background light.

lator are small, particularly at modulation frequencies above 1 kHz. Maximum phase variations of  $0.5^{\circ}$  at 1.5 kHz and  $0.1^{\circ}$  at 3 kHz were observed during a 10-min period. Below 1 kHz, with incomplete or square-wave-like modulation, a phase stability of about  $1^{\circ}$  during a similar period can be obtained. A time resolution of  $\pm 10$  nsec can readily be achieved at the upper end of the modulation frequency range [2].

## • Elimination of stray light

The stray light problem in this experiment is less severe than in a standard flash spectroscopic experiment since the exciting source has only a few discrete emission lines rather than a broad continuous spectrum. Thus most stray light can be eliminated by the monochromator. However, any stray light that reaches the detector produces a much larger signal than would the same amount of background light because the former is fully modulated while the latter is modulated only to a small extent.

Several alternative methods have been used successfully for stray-light elimination. Addition of optical transmission-filter materials to the cooling water has already been mentioned. At a modulation frequency high enough to produce a significant phase shift, the absorption spectrum of a transient can be recorded out of phase with unwanted stray and short-lived fluorescence emission signals. A suppression by about two orders of magnitude can thus be achieved. However, since only one component of the absorption signal is measured, its absolute value and phase shift cannot be determined by such a measurement alone.

Light baffles inside the absorption cell, in the form of a blackened brass spiral with thin flat turns, were found to decrease stray light by about an order of magnitude, while decreasing the excitation of the cell volume by a factor of only two or three. Another effective method for rejecting stray light is double modulation, which is discussed in the following section.

# • Separation of emission and absorption signals by double modulation

If only the exciting source is modulated, stray light and fluorescence emission from the reaction cell can be eliminated by subtracting the modulation spectrum obtained with the background source blocked off from the spectrum recorded with the background source turned on. The former spectrum has a high signal-to-noise ratio and represents only stray and emission signals; the latter has a low signal-to-noise ratio and contains the absorption signal as well. This process is often unsatisfactory because of slow drifting of both signals in time, caused mainly by deposition of reaction products. The problem can be eliminated by rapid alternation between emission and absorption measurements, i.e., by chopping the background light, sorting out the two measurements with a synchronous alternator, filtering them separately, and measuring their difference with an appropriate amplifier. This procedure is different from the one normally applied in double-beam optical spectrometers; it makes possible the use of unequal on and off periods, which are necessary to take into account the unequal signal-to-noise ratios of the two measurements.

A circuit designed to perform this function was operated at 5 Hz with a chopping ratio of about 8:1 for background on: off time [32]. Figure 10 shows its performance when applied to a portion of the triplet naphthalene absorption spectrum, which is partly obscured by naphthalene fluorescence emission when recorded in phase with the exciting light. It should be noted that the pure absorption spectrum is recovered without a significant decrease in S/N.

# • Spurious absorption signals

Since absorption is measured as a modulation of the background light beam, any other process that causes the beam to be modulated coherently with the exciting light will be mistaken for an absorption signal. Spurious signals of this type can be generated by vibration of optical and other components touched by the background light beam. It appears that coherent vibrations can be excited by sound waves produced by the modulated Hg arc.

This type of signal was generally found to be weak, equivalent to an absorption of  $10^{-5}$  or less for modulation frequencies down to 80 Hz. It is often not feasible to test the origin of weak signals by stopping the reactant flow. Instead, a test can be made by adding enough colloidal graphite to the lamp coolant to make it opaque. A spurious signal will persist, but transient absorption will disappear.

# • Direct recording of absorption

Since transient absorption in this experiment is small and usually less than  $10^{-2}$ , the ratio of ac to dc photocurrent is a direct measure of rms absorption. This ratio can be obtained directly by using an analog divider. Alternatively, a feedback circuit can be used that keeps the dc photocurrent constant by changing the photomultiplier voltage. In this way an artificial constant-intensity background is obtained. The feedback loop must be designed to compensate for the slow variations in background intensity without attenuating the modulation signal. Figure 11 shows a triplet naphthalene absorption band located in the falloff region of the Xe arc spectrum; distortions of the band shape and shift of the absorption maximum, caused by a rapid variation of background intensity, were eliminated by using the constant-background circuit [32].

# Results

# • First-order decay kinetics

A simple example of a pseudo-first-order reaction is the decay of Hg  $(6^3P_0)$  atoms in the presence of a quenching gas; this process is described by the reaction sequence (1), (2) and (3). The time-dependent concentration of metastable atoms in  $N_2$ , at sufficiently high pressure, follows Eq. (5) since formation of the metastable state, step (2), is much faster than its decay, step (3). Atoms in the  $6^3P_0$  state can be monitored in absorption using the transitions  $6^3D_1 \leftarrow 6^3P_0$  at 296.7 nm and  $7^3S_1 \leftarrow 6^3P_0$  at 404.7 nm.

For a quenching reaction according to (3), the decay rate of metastable atoms should be linearly dependent on the concentration of the quencher  $M(S_0)$  and should not depend on the modulation frequency. This behavior is shown in Fig. 12 for quenching by naphthalene vapor. The decay rate changes linearly with naphthalene pressure, as expected, except for some curvature at the lowest concentrations. This curvature can be shown to be due to decomposition of naphthalene, with an estimated quantum yield of  $5 \times 10^{-4}$ . The linear part of the plot corresponds to a quenching rate constant of  $(2.75 \pm 0.06) \times 10^{11}$  l-mole<sup>-1</sup>-sec<sup>-1</sup>, or an effective cross section of  $0.5 \pm 0.01$  nm<sup>2</sup> [1]. The intercept of the curve at zero naphthalene pressure represents the decay rate of  $Hg(^3P_0)$  atoms in pure  $N_2$ , measured as  $(8.9 \pm 0.1) \times 10^3$  sec<sup>-1</sup>.

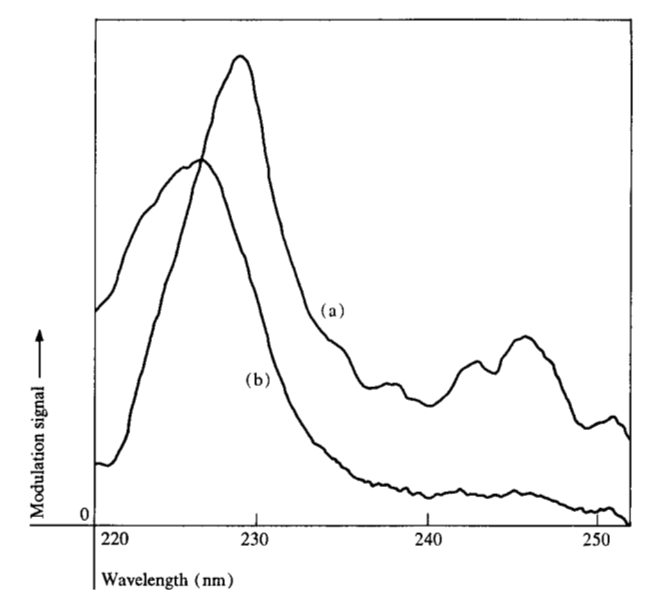
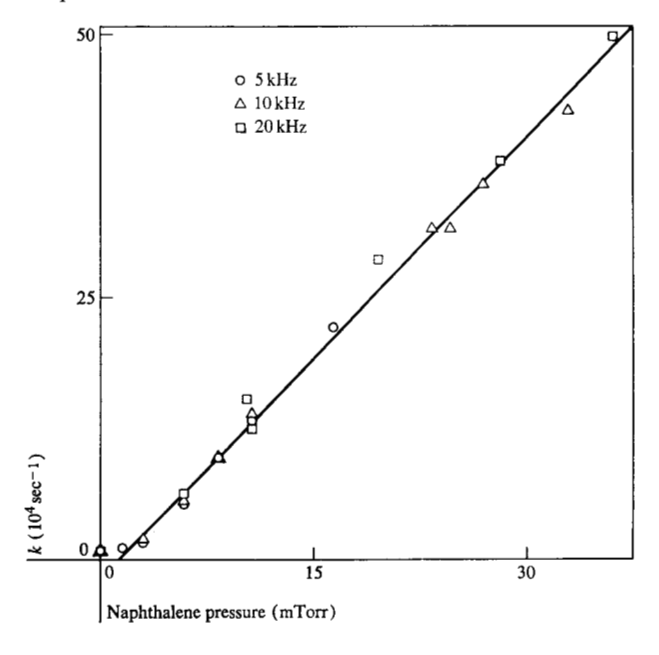


Figure 11 Effect of constant background circuit for triplet naphthalene band at 227 nm: (a) Modulation signal obtained with a constant photomultiplier voltage. (b) The same signal recorded using the constant background circuit.

Figure 12 Rate of quenching of  $Hg(6^{a}P_{o})$  atoms by naphthalene vapor, in 780 Torr  $N_{o}$ . The phase shift of the 296.7-nm absorption line was measured at three modulation frequencies.



Another example of first-order kinetics is the fluorescence decay of benzene vapor in an atmosphere of inert gas. Benzene can be excited directly to the  $^{1}B_{2u}$  electronic level by absorption of 253.7-nm radiation and fluorescence occurs predominantly from the vibrational ground state

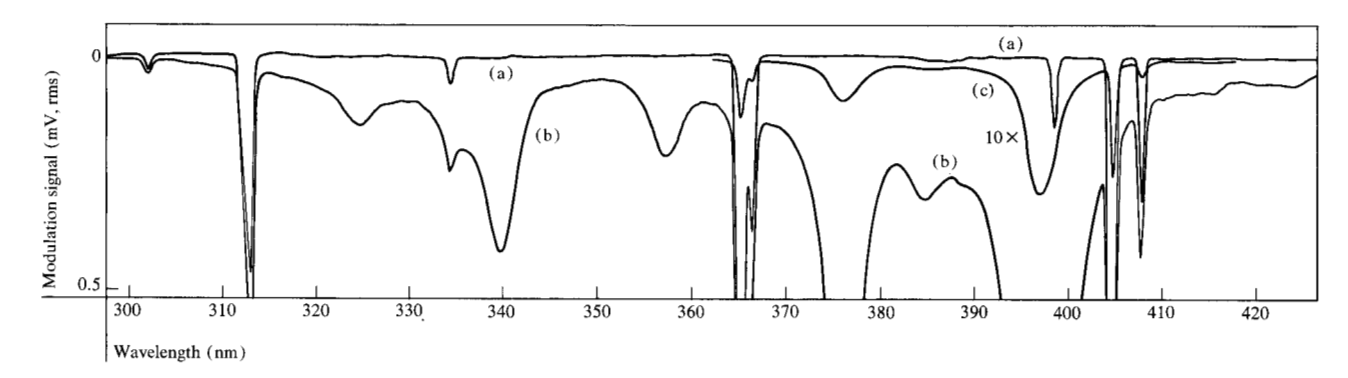


Figure 13 Triplet naphthalene absorption spectrum, recorded with a Xe background light source, out of phase with the naphthalene fluorescence: (a) Background source off; (b) and (c), background source on. The sensitivity for trace (c) was a factor of ten lower than for trace (b). Experimental conditions: spectral slit width, 0.8 nm; modulation frequency, 990 Hz; pressures—naphthalene, 40 mTorr; Hg, 0.3 mTorr; N<sub>2</sub>, 800 Torr.

of this level at sufficiently high inert-gas pressure. Phase-shift measurements at 150 kHz with 3 to 10 Torr of benzene vapor in 760 Torr of  $N_2$  or Ar yielded a lifetime of  $80 \pm 10$  nsec, which was independent of the benzene pressure [2]. This result is in agreement with other recent observations [41, 42].

Measurements of this type are known as phase fluorometry [24]. The example given demonstrates that the modulated Hg arc is suitable for phase fluorometry of vapors. Compared with other experiments of this type, it has the disadvantages of poor time resolution and fixed excitation wavelength, but the advantage of a spectral width for excitation *and* emission sampling that can be made very narrow, due to the high power in the 253.7-nm source line.

# • Triplet-state absorption spectra

As indicated in the introduction, the main objective in developing this technique was its application to optical spectroscopy of triplet states in the gas phase. A simple test example was naphthalene, which is one of the few molecules whose gas-phase triplet absorption spectra are known [5]. It was observed that the quenching of  $Hg(6^3P_0)$  atoms by naphthalene vapor, discussed above, did indeed produce triplet naphthalene with high efficiency, as implied by (3). The possibility that quenching produces an excited singlet state, which then undergoes intersystem crossing, was ruled out on the basis of observations on the naphthalene fluorescence emission.

Figure 13 shows a scan of the triplet naphthalene absorption spectrum obtained by Hg photosensitization. This is the part of the spectrum that had been observed previously by flash spectroscopy [7]. The five strongest bands agree with the earlier observations and were detected with a high signal-to-noise ratio. In addition, some weaker, new bands were also observed. A list of the peak wavelengths

and a discussion of the weaker absorptions have been given previously [1].

Some features of the experiment discussed earlier are illustrated by Fig. 13. The naphthalene fluorescence emission in the range 310 to 360 nm (compare Fig. 10) was eliminated from this spectrum by proper phase adjustment of the detector; i.e., the component of the absorption spectrum out of phase with the fluorescence was recorded. The result is similar to the one obtained by double modulation, as shown in Fig. 10, except for the relative sign of absorption and Hg-stray-light lines. Because of a delayed fluorescence component, these lines also appear in the out-of-phase spectrum. The phase relationships are explained by the phase diagram in Fig. 14. Since the Hg lines are narrow and few in number they do not significantly disturb the spectrum of the molecular species. In fact, they are useful for wavelength calibration.

An absorption spectrum of triplet biphenyl (Fig. 15) was obtained in an analogous way. This band has not been observed before in the gas phase. However, observations in the liquid and solid phases were made by a number of investigators [43]. Comparison with the gas-phase spectrum reveals an unusually large solvent shift. The band maximum is found at 333 nm in the gas and at 361 to 375 nm in the condensed phase. This observation probably indicates that the upper state involved in this transition undergoes a strong solvent interaction. The spectrum of Fig. 15 also shows the drastic effect of the sensitizing Hg vapor on the triplet concentration. The weaker trace was taken without Hg flowing through the absorption cell. When Hg vapor was admitted, the strong absorption spectrum was obtained.

The triplet absorption spectra discussed so far can also be observed by the flash spectroscopic technique, at least in the liquid or solid phase. However, this is not feasible in the following cases. It can be seen from the naphthalene

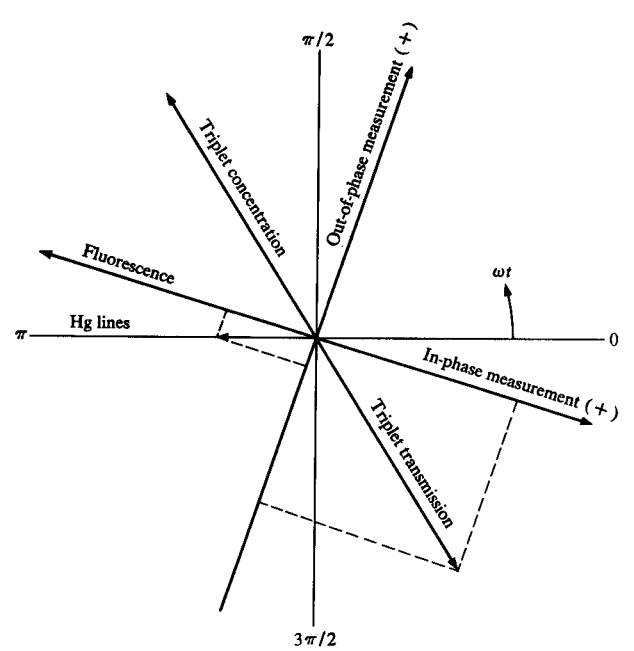
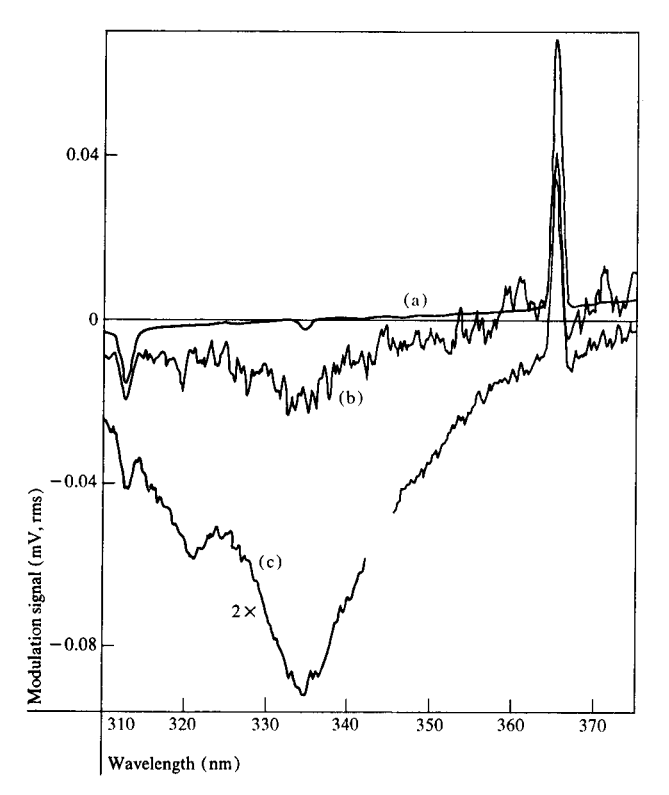


Figure 14 Phase diagram for the triplet naphthalene spectra of Figs. 10 and 13.

Figure 15 Triplet biphenyl absorption spectrum: (a) Background source off; (b) background source on,  $N_2$  and biphenyl flowing; (c) same as (b) but Hg also flowing. The sensitivity for trace (c) was a factor of two lower than for trace (b). Experimental conditions; Xe background source; spectral slit width, 1.4 nm; modulation frequency, 1.4 kHz; pressures—biphenyl, 8 mTorr; Hg, 0.3 mTorr;  $N_2$ , 360 Torr.



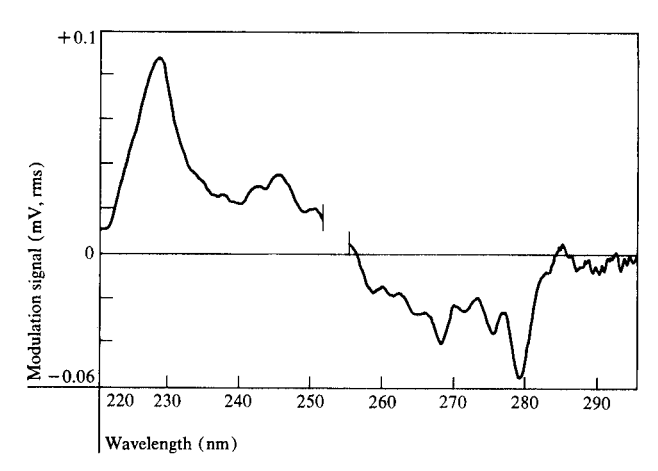


Figure 16 Short-wavelength triplet-absorption and ground-state-depopulation spectrum of naphthalene. Experimental conditions: Xe background source; spectral slit width, 1.4 nm; modulation frequency, 1 kHz; pressures—naphthalene, 8 mTorr; Hg, 0.3 mTorr; N<sub>2</sub>, 500 Torr.

quenching curve for metastable Hg atoms, Fig. 12, that almost complete energy transfer by Hg photosensitization is possible at very low pressure, i.e., at a concentration of the quenching molecules low enough to leave the wavelength range of their ground-state absorption spectrum essentially transparent. Thus it is possible to observe triplet absorption bands that are located within the range of the ground-state absorption spectrum.

An example of such an observation is given in Fig. 16, which shows the modulation spectrum of naphthalene vapor in the presence of Hg vapor in the 220- to 300-nm wavelength range. The positive band appearing to the left of the 253.7-nm exciting line is a new triplet absorption band, predicted by calculations to be a strongly allowed transition and to occur near 217 nm [44]. The negative spectrum to the right of the exciting line is the groundstate depopulation spectrum of naphthalene. It appears with opposite sign because it is 180° out of phase with the triplet absorption signal, the ground state being depopulated as the triplet state is populated. Since the two spectra do not overlap significantly, and the ground state extinction coefficients can be measured easily under identical conditions, an estimate of the triplet-band extinction coefficient can be obtained by comparing the two signals. Our estimate is  $\epsilon_{227} = 7.3 \times 10^4 \text{ l-mole}^{-1}\text{-cm}^{-1}$ , which confirms the strongly allowed nature of the band. The spectrum of Fig. 16 is not corrected for the intensity of the Xe background source, which drops sharply with wavelength in this region. A trace of the triplet band corrected for this effect was shown in Fig. 11. The true maximum is located at 227 nm.

Benzene is an outstanding example of a case in which ground-state absorption interferes with the detection of

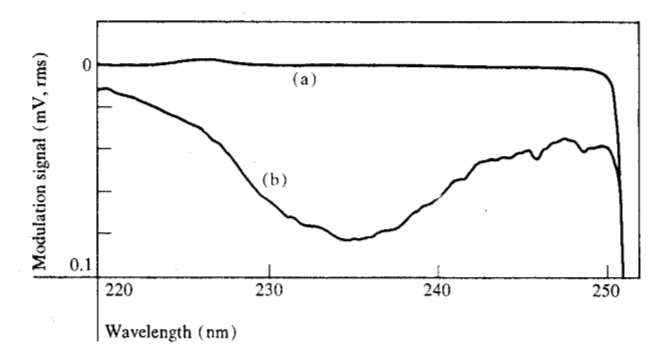
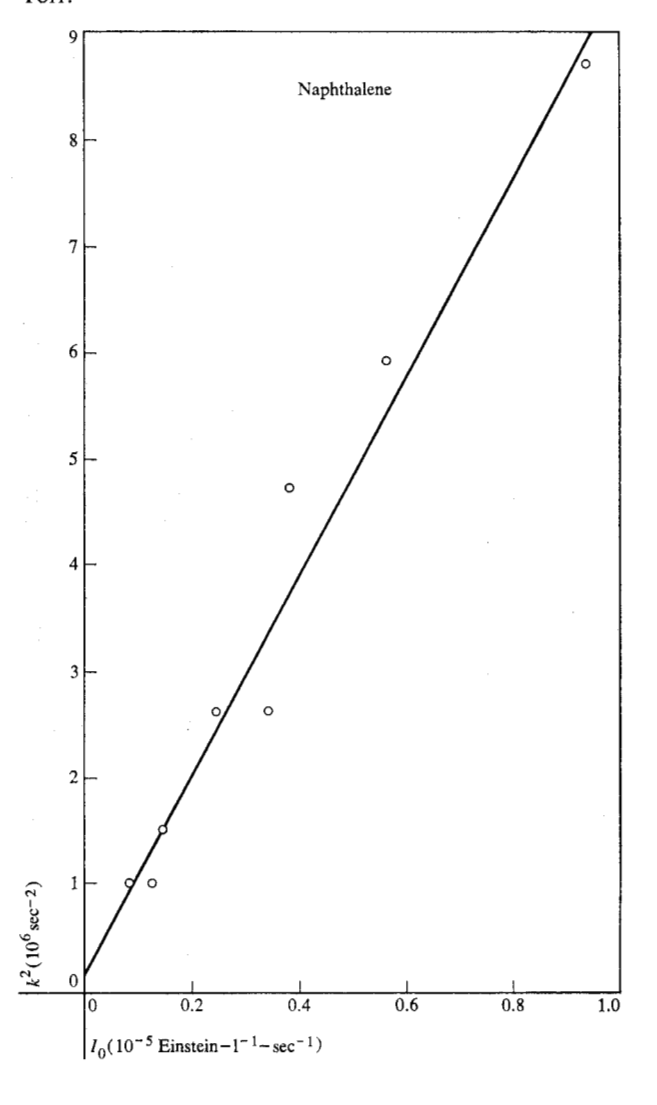


Figure 17 Triplet absorption spectrum of benzene-d<sub>0</sub>: (a) Background source off; (b) background source on. Experimental conditions: Xe background source; spectral slit width, 3.2 nm; modulation frequency, 1.45 kHz; pressures—benzene-d<sub>0</sub>, 120 mTorr; Hg, 0.3 mTorr; N<sub>2</sub>, 315 Torr.

Figure 18 Second-order decay of triplet naphthalene. The squares of apparent first-order rate constants are plotted vs the dc excitation rate  $I_0$ . Experimental conditions: monitoring wavelength, 397 nm; modulation frequency, 330 Hz; pressures—naphthalene, 20 mTorr; Hg, 0.3 mTorr;  $N_2$ , 450 Torr.



a triplet-triplet transition. Calculations restricted to the  $\pi$ -electron system predict only one allowed transition from the lowest triplet state to another triplet state below the ionization limit. This transition is of the type  ${}^3E_{2g}^+ \leftarrow {}^3B_{1u}^-$  and is estimated to occur at 260 to 234 nm [45, 46]. The corresponding absorption band has often been searched for under a variety of conditions, but only in a solid glass at low temperature has some indication of it been found. The feature observed was very diffuse, with an uncertain maximum at 240 nm, and extended beyond 300 nm toward the visible wavelengths [47].

With the Hg-photosensitization technique, transient absorption bands were found for benzene, benzene-d6 and toluene in the region predicted for the allowed triplettriplet transition [3]. The modulation signal observed between 220 and 250 nm with benzene-d<sub>6</sub> is shown in Fig. 17. It was also independently confirmed by the biacetyl technique [48] that triplet benzene is produced by the Hg-photosensitization process. Extinction coefficients at the maxima of the transient bands were estimated from the absorption amplitudes, observed under conditions as similar as possible to those of actinometric measurements. Homogeneous excitation of the cell volume was assumed. The results were, in  $1-\text{mole}^{-1}-\text{cm}^{-1}$ , 3  $\times$  10<sup>3</sup> for benzene and  $1.5 \times 10^3$  for toluene. These figures, in conjunction with the band shapes, yielded experimental oscillator strengths of about 0.06 for all three molecules, which is in satisfactory agreement with a value of 0.09 calculated recently for the  ${}^{3}E_{2g}^{+} \leftarrow {}^{3}B_{1u}^{-}$  transition [46].

## • Second-order decay kinetics

Decay of aromatic hydrocarbon triplets by the process of triplet-triplet "annihilation" is a good example of second-order kinetics. The theory of measuring second-order decay rates by the modulation technique has been discussed in a previous section of this paper. It requires the determination of an apparent first-order rate constant k as a function of the constant part of the intensity of excitation,  $I_0$ . This latter parameter was varied in the experiment in a stepwise manner by adding a neutral-density filter solution (colloidal graphite) to the lamp coolant. The absolute value of  $I_0$  was calculated from the expression

$$I_0 = A\omega(1 + \tan^2\phi)^{\frac{1}{2}}/(2.3 \epsilon l\alpha \tan\phi),$$
 (17)

where  $\alpha = I_1/I_0$  is the degree of modulation as determined by a separate measurement, A is the observed absorption amplitude, I is the absorption path length (60 cm), and  $\epsilon$  is the triplet extinction coefficient at the observation wavelength. Equation (17) is readily derived from Eq. (5) by noting that, for small absorption,  $A = 2.3 \epsilon lc$ .

Application of this method to the decay of triplet naphthalene led to the results shown in Fig. 18. The extinction coefficient used for the maximum of the 397-nm

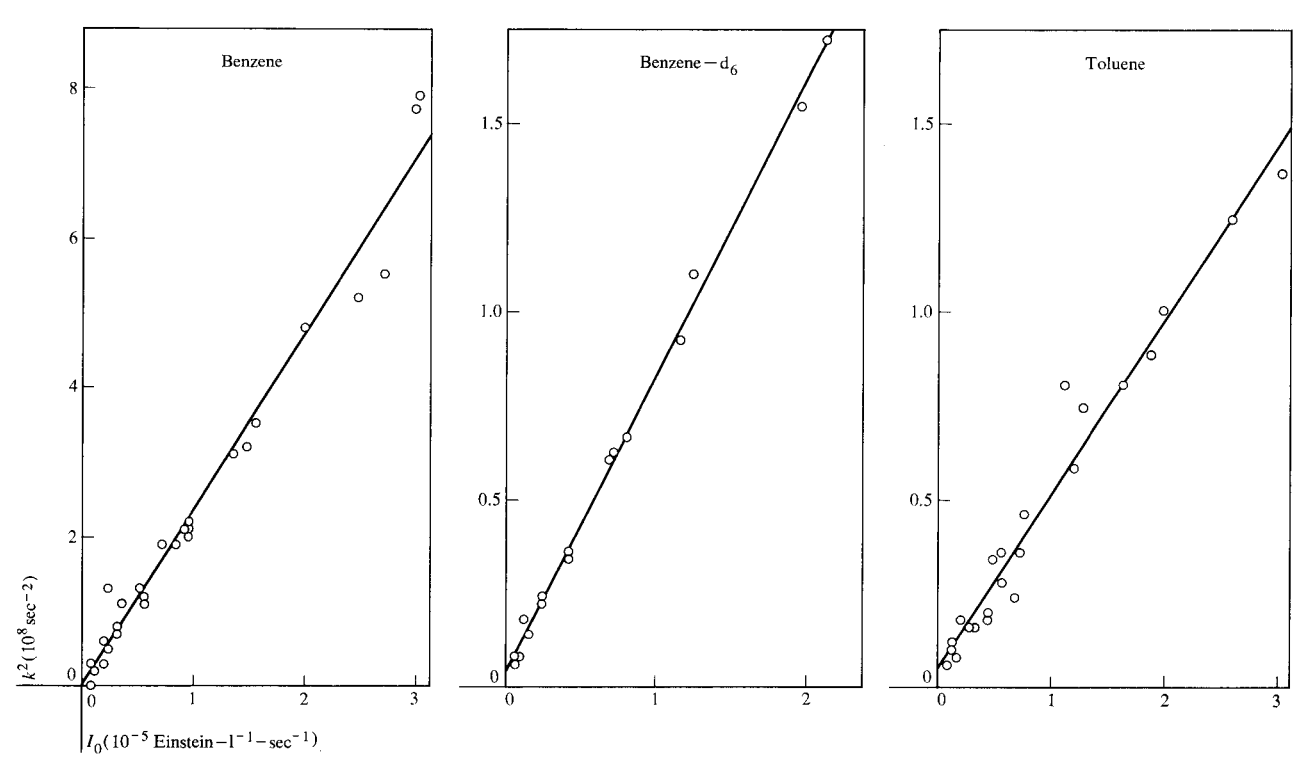


Figure 19 Second-order decay of triplet benzene, benzene- $d_6$  and toluene. The squares of apparent first-order rate constants are plotted vs the dc excitation rate  $I_0$ . Experimental conditions: monitoring wavelengths, 235 nm for benzene and 242 nm for toluene; modulation frequency, 2 kHz; pressures—benzene and toluene, 300 mTorr; Hg, 0.3 mTorr;  $N_2$ , 350 Torr.

band of triplet naphthalene was  $3.7 \times 10^4$ , estimated as described above for benzene and toluene. A least-squaresfit straight line through the experimental points yielded the first- and second-order rate constants  $k_1 = (4.3 \pm 3.7)$  $\times 10^2 \text{ sec}^{-1}$  and  $k_2 = (2.4 \pm 0.2) \times 10^{11} \text{ l-mole}^{-1} \text{-sec}^{-1}$ , respectively. This value of  $k_2$  is close to the value (2.3  $\pm$  $0.3) \times 10^{11} \text{ l-mole}^{-1}\text{-sec}^{-1}$  derived from the flash spectroscopic experiment [49] by using the same extinction coefficient [50]. The first-order rate constant is determined primarily by  $O_2$  impurity quenching. A value for  $k_1$  of  $3 \times 10^2 \text{ sec}^{-1}$  was estimated for this process from the typical  $O_2$  content (8  $\times$  10<sup>-6</sup> mole-percent) of the  $N_2$ used and a rate constant for O2 quenching of triplet naphthalene determined by flash spectroscopy [49]. Considerable scatter of the data in Fig. 18 is due to the poorer phase stability of the Hg arc below 1 kHz.

The transient bands observed with benzene and toluene, which were ascribed to the lowest triplet states of these molecules, led to the first direct observation of the decay kinetics of these species in the gas phase. This observation is of particular interest, since indirect observations had led to the conclusion that triplet benzene showed an anomalous behavior, decaying unimolecularly at a rate of about  $10^5 \text{ sec}^{-1}$  at 300°K under these conditions [51, 52]. Measurements analogous to those described for naphthalene are shown in Fig. 19. They indicate clearly that the pre-

sumed anomalous behavior is absent. The zero-intensity intercepts yielded first-order-decay rate constants  $k_1^2 = (-1 \pm 10) \times 10^6 \text{ sec}^{-2}$  for benzene,  $k_1 = (2.0 \pm 0.2) \times 10^3 \text{ sec}^{-1}$  for benzene-d<sub>6</sub>, and  $k_1 = (2.3 \pm 0.5) \times 10^3 \text{ sec}^{-1}$  for toluene, all of which can be explained as quenching of the triplet states by residual O<sub>2</sub> and normal hydrocarbon molecules [3]. The second-order rate constants, which were tentatively interpreted as being due to triplet-triplet annihilation, were found to be extremely large, being (in l-mole<sup>-1</sup>-sec<sup>-1</sup>)  $k_2 = (5.8 \pm 0.6) \times 10^{12}$  for benzene,  $k_2 = (2.0 \pm 0.2) \times 10^{12}$  for benzene-d<sub>6</sub>, and  $k_2 = (1.1 \pm 0.1) \times 10^{12}$  for toluene.

#### Outlook

The results obtained so far, and summarized in the previous section, show that the technique of modulated Hgphotosensitization is a valuable tool for the observation of triplet states in the gas phase. Another observation in gas-phase kinetics and spectroscopy that can be made using the modulated Hg arc as an excitation source is the determination of reaction rates for neutral atoms. Hydrogen and oxygen atoms can be generated by Hgphotosensitized reactions in the following way [9,15]:

$$Hg(^{3}P_{1}) + H_{2} \rightarrow HgH + H$$

$$Hg(^{3}P_{1}) + N_{2}O \rightarrow N_{2} + O + Hg(^{1}S_{0}).$$

The rates at which these atoms react with another gas can be measured either by monitoring their concentrations directly, using their vacuum uv resonance absorption lines and Eq. (5), or by observing a product absorption band and applying Eq. (6).

The modulated Hg arc technique should also be applicable to the measurement of rates of radical reactions in the gas phase. It is well known, for instance, that saturated hydrocarbons produce radicals in Hg-photosensitized reactions [9] according to the general scheme

$$Hg(^{3}P_{1}) + RH \rightarrow \dot{R} + Hg(^{1}S_{0}) + \dot{H}.$$

For many Hg-photosensitized reactions intermediate states have been proposed whose existence and kinetics could be investigated by the technique described here. Two examples are the HgCO\* molecule proposed by Homer and Lossing [53],

$$Hg(^{3}P_{1}) + CO \rightarrow HgCO^{*},$$

and the cyclopropene-carboxyaldehyde intermediate species in the Hg-photosensitized decomposition of furan proposed by Srinivasan [54],

We have also noted that in a mixture of Hg vapor and  $N_2$ , the second metastable state of the Hg atom,  $6^3P_2$ , is populated, presumably by stepwise excitation in the presence of 404.7-nm radiation:

$$Hg(6^{3}P_{0}) \xrightarrow[\text{absorption}]{404.7 \, \text{nm}} Hg(7^{3}S_{1}) \xrightarrow[\text{emission}]{546.1 \, \text{nm}} Hg(6^{3}P_{2}).$$

Measurements of the quenching of this state by various gases would be valuable for a better understanding of the factors governing the reaction rates of the different spin states of the  $6^3P$  term of the Hg atom. There is a large difference in reactivity between the  $6^3P_1$  and the  $6^3P_0$  states for some gases [8], and virtually none for others [1]. No satisfactory explanation of this effect has been found.

Finally, the technique described here could be extended to photosensitization by other metal atoms, especially Cd and possibly Zn. On the one hand this is experimentally more difficult, since a temperature of 250 to 300°C is necessary to establish a sufficient vapor pressure of Cd. On the other hand an advantage lies in the fact that, with Cd, the triplet states of some molecules, such as  $C_2H_4$ , can be efficiently populated without accompanying decomposition, a complication that arises when Hg is used [55].

# **Acknowledgments**

Thanks are due A. Halperin for his enthusiastic help in developing the electronic instrumentation. A major part of the work reported was done in collaboration with C. S. Burton, who also suggested improvements of the manuscript, and with the skillful technical assistance of H. R. Wendt. Discussions with R. J. Cvetanovic, F. P. Lossing, G. V. Michael, R. Srinivasan, J. S. Wilczynski and C. B. Zarowin are gratefully acknowledged.

# **Appendix**

It is useful to consider the heating effect in a cylindrical gas volume caused by radiation as described by Eq. (4). First, the gas temperature will differ from that of the enclosure and will be nonuniform. Second, a periodic variation of temperature will occur which can, in principle, cause a modulation of the normal absorption spectrum of a gas by periodic population changes of vibrational and rotational energy levels. Temperature modulation effects in infrared absorption spectra due to periodic compression of the gas have been observed by phasesensitive detection of the changes in the spectrum [21].

A simple model for these effects consists of a cylinder of infinite length, radius  $r_0$  and surface temperature  $T_s$ , filled with an incompressible "gas" of heat capacity  $\gamma$  (per-unit-volume) and thermal conductivity  $\kappa$ . Heat is generated homogeneously as described by Eq. (4). [If the heat release is delayed by slow decay of a metastable species, Eq. (4) has to be modified accordingly.] The time-dependent radial temperature distribution in this model can be formulated as

$$T(r, t) = T_0(r) + T_1(r) \exp(i\omega t), \tag{A1}$$

with  $0 \le r \le r_0$ . Solution of the heat transport equation yields the following expressions for  $T_0$  and  $T_1$ :

$$T_0 = T_s + I_0(r_0^2 - r^2)/4\kappa \tag{A2}$$

and

$$T_{1} = \frac{iI_{1}}{\gamma\omega} \left[ \frac{J_{0}^{*}(xi^{\frac{1}{2}})}{J_{0}^{*}(x_{0}i^{\frac{1}{2}})} - 1 \right], \tag{A3}$$

where  $x = r(\gamma \omega/\kappa)^{\frac{1}{2}}$ ,  $x_0 = r_0(\gamma \omega/\kappa)^{\frac{1}{2}}$  and  $J_0^*$  is the complex conjugate of the zeroth-order Bessel function of the first kind [56]. For high frequencies Eq. (A3) becomes

$$T_1 = -iI_1/\gamma\omega, \quad (x_0 \to \infty);$$
 (A4)

and for low frequencies,

$$T_1 = I_1(r_0^2 - r^2)/4\kappa, \quad (x_0 \to 0).$$
 (A5)

The temperature difference between the cylinder axis and wall is  $\Delta T = I_0 r_0^2 / 4\kappa$ . For the experimental conditions  $r_0 = 0.016$  m and  $I_0 = 6 \times 10^4$  W-m<sup>-3</sup>,  $\Delta T = 25$ °K for He and 140°K for N<sub>2</sub> [57]. These temperature differences are, however, attenuated by convection, influx

of cool gas, and enhanced light absorption near the cylinder wall

In Fig. A1 the in-phase (Re  $T_1$ ) and out-of-phase (Im  $T_1$ ) parts of the alternating temperature described by Eq. (A3) are plotted vs the reduced radius  $x/x_0$ . As  $x_0$  varies from 1 to 10, the behavior of  $T_1$  changes from being close to the low frequency limit, Eq. (A5), to a predominantly adiabatic heating, as described by Eq. (A4), except for regions close to the wall. At the same time, the phase shift of  $T_1$  changes gradually from 0 to  $-90^\circ$ .

Under typical experimental conditions the amplitude of  $T_1$  is small and the adiabatic limit of Eq. (A4) is approximated closely. At a pressure of 300 Torr, a modulation frequency of 50 Hz, and other conditions as given previously, one finds  $x_0 = 10$ ,  $I_1/\gamma \omega = 1.0$ °K for He and  $x_0 = 31$ ,  $I_1/\gamma\omega = 0.6$ °K for N<sub>2</sub>. Temperature modulation of the normal absorption spectrum of a molecule is therefore expected only at low modulation frequencies, low gas pressures and high intensities. For an order-ofmagnitude estimate of this effect, consider a molecule with two nondegenerate energy levels at E = 0 and E = kT. The fractional depletion of the lower level, caused by a temperature variation  $\delta T$ , is  $0.20 \delta T/T$ . If molecules in the lower level absorb, say, 30 percent of the light at a particular wavelength, a variation of  $-1.6 \times$  $10^{-4}$  in absorption would be caused by  $\delta T = +1$ °K at T = 300°K. As mentioned before, such a change would be detectable. However, detection requires that the absorption spectra of molecules in the upper and lower levels be sufficiently distinct, which is often not the case.

# References and notes

- 1. H. E. Hunziker, Chem. Phys. Letters 3, 504 (1969).
- C. S. Burton and H. E. Hunziker, J. Chem. Phys. 52, 3302 (1970).
- C. S. Burton and H. E. Hunziker, Chem. Phys. Letters 6, 352 (1970).
- S. P. McGlynn, T. Azumi and M. Kinoshita, Molecular Spectroscopy of the Triplet State, Prentice-Hall, Inc., Englewood Cliffs, N. J. 1969.
- The Triplet State, edited by A. B. Zahlan, Cambridge University Press, London 1967.
- G. Porter and M. W. Windsor, Proc. Roy. Soc. (London) A245, 238 (1958).
- G. Porter and F. J. Wright, Trans. Faraday Soc. 51, 1205 (1955).
- A. B. Callear and G. J. Williams, Trans. Faraday Soc. 60, 2158 (1964).
- R. J. Cvetanovic, in *Progress in Reaction Kinetics*, edited by G. Porter, the Macmillan Co., New York 1964, p. 41.
- 10. J. G. Calvert and J. N. Pitts, Jr., *Photochemistry*, John Wiley and Sons, Inc., New York 1967, p. 92.
- E. W. R. Steacie, Atomic and Free Radical Reactions, 2nd Ed., Vol. I, Reinhold Publishing Corp., New York 1954, p. 411.
- 12. K. J. Laidler, J. Chem. Phys. 15, 712 (1947).
- G. Porter, in *Techniques of Organic Chemistry*, edited by S. L. Friess, E. S. Lewis and A. Weissberger, 2nd Ed., Vol. III, Part II, Interscience Publishers, Inc., New York 1961, Chap. XIX.

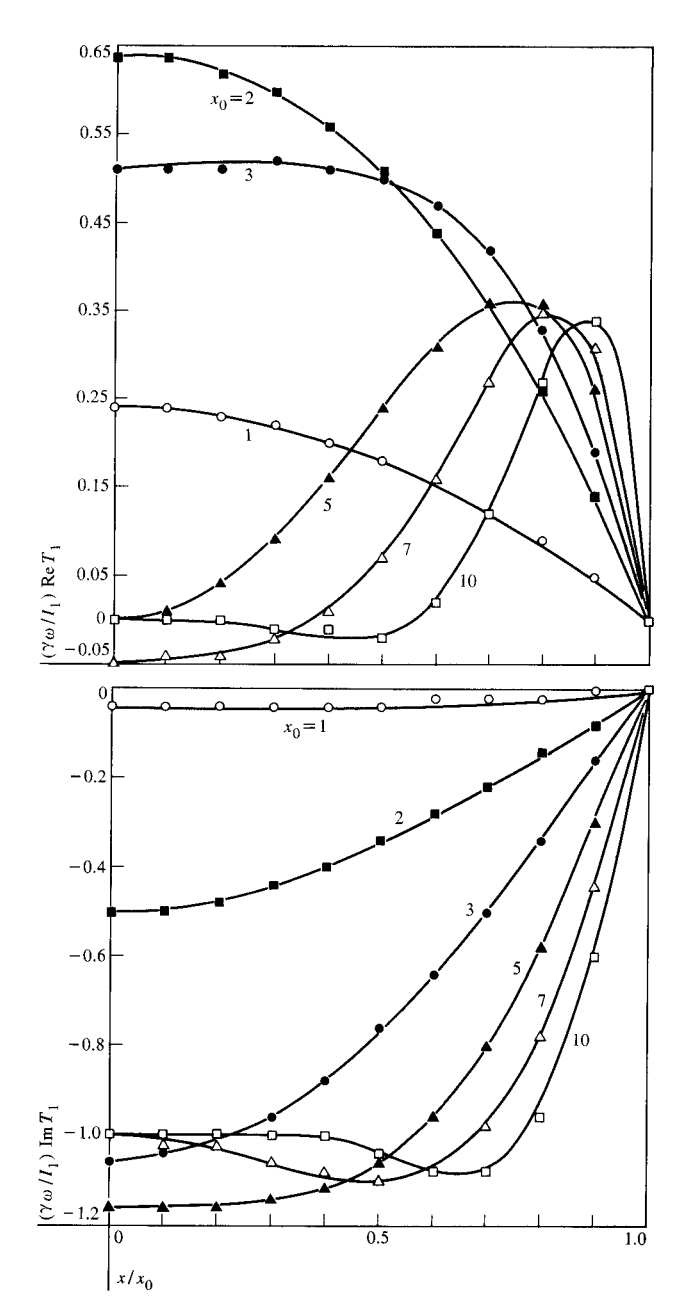


Figure A1 In-phase (top) and out-of-phase (bottom) parts of the temperature modulation in a cylindrical absorption cell [calculated from Eq. (A3)] as a function of the reduced cell radius.

- A. B. Callear and R. E. M. Hedges, *Nature* 218, 163 (1968).
- 15. A. B. Callear and J. McGurk, Nature 226, 844 (1970).
- 16. Ref. 10, p. 696.
- H. S. Johnston, G. E. McGraw, T. T. Paukert, L. W. Richards and J. van den Bogaerde, *Proc. Natl. Acad. Sci. U. S.* 57, 1146 (1967).
- 18. H. Labhart, Helv. Chim. Acta 47, 2279 (1964).
- D. J. Dyson and M. A. Slifkin, J. Sci. Instr. 40, 599 (1963).
- 20. R. M. Hexter, J. Opt. Soc. Am. 53, 703 (1962).

25

- J. C. Gilfert and D. Williams, J. Opt. Soc. Am. 48, 765 (1958).
- 22. E. J. Bair, J. T. Lund and P. C. Cross, *J. Chem. Phys.* **24**, 961 (1956).
- R. A. Smith, F. E. Jones and R. P. Chasmar, The Detection and Measurement of Infrared Radiation, Oxford University Press, London 1957, pp. 191, 290.
- J. B. Birks and F. H. Munro, in *Progress in Reaction Kinetics*, edited by G. Porter, Vol. IV, The Macmillan Co., New York 1967, p. 239.
- E. Kamke, Differentialgleichungen Reeller Funktionen,
   3d Ed., Akademische Verlagsgesellschaft Geest & Portig
   K. -G., Leipzig 1956, p. 41.
- 26. A. H. Pfund, Science 90, 326 (1939).
- 27. J. U. White, J. Opt. Soc. Am. 32, 285 (1942).
- 28. J. Strong, Concepts of Classical Optics, W. H. Freeman Co., San Francisco 1958, p. 346.
- B. Budick, R. Novick and A. Lurio, Appl. Optics 4, 229 (1965).
- F. X. Powell, O. Fletcher and E. R. Lippincott, Rev. Sci. Instr. 34, 36 (1963).
- Similar generators are available commercially, e.g., Model T-5-3-XC-MC-S, Lepel High Frequency Laboratories, New York, N. Y.
- 32. Circuit diagrams are available from the author on request.
- 33. M. Kasha, J. Opt. Soc. Am. 38, 929 (1948).
- 34. R. Feldtkeller, *Vierpoltheorie*, 7th Ed., S. Hirzel Verlag, Stuttgart 1959, p. 127.
- 35. F. P. Lossing, D. G. H. Marsden and J. B. Farmer, *Can. J. Chem.* 34, 701 (1956).
- 36. Reference Data for Radio Engineers, 5th Ed., H. W. Sams & Co., Inc., Indianapolis 1968, p. 6-1.
- A. C. G. Mitchell and M. W. Zemansky, Resonance Radiation and Excited Atoms, Cambridge University Press, London 1961, p. 230.
- 38. Ref. 37, p. 169.
- D. W. Setser, B. S. Rabinovitch and D. W. Placzek, J. Am. Chem. Soc. 85, 862 (1963), and earlier references given therein.
- R. J. Cvetanovic, H. E. Gunning and E. W. R. Steacie, J. Chem. Phys. 31, 573 (1959).
- 41. M. Nishikawa and P. K. Ludwig, J. Chem. Phys. 52, 107 (1970).

- 42. B. K. Selinger and W. R. Ware, J. Chem. Phys. 52, 5482 (1970).
- 43. Y. H. Meyer, R. Astier and J. M. Leclercq, *Chem. Phys. Letters* 4, 587 (1970), and earlier references given therein.
- 44. R. L. de Groot and G. J. Hoytink, J. Chem. Phys. 46, 4523 (1967).
- 45. R. Pariser, J. Chem. Phys. 24, 250 (1956).
- 46. S. de Bruijn, Chem. Phys. Letters 5, 428 (1970).
- 47. T. S. Godfrey and G. Porter, *Trans. Faraday Soc.* **62**, 7 (1966).
- 48. H. Ishikawa and W. A. Noyes, *J. Chem. Phys.* 37, 583 (1962).
- G. Porter and P. West, Proc. Roy. Soc. (London) A279, 302 (1964).
- 50. An earlier value,  $k_2 = (3.4 \pm 0.3) \times 10^{11}$  1-mole<sup>-1</sup>-sec<sup>-1</sup>, given in Ref. 3 for the rate constant of triplet naphthalene, was found to be too high because 253.7-nm stray light had been used for the phase reference at a naphthalene pressure not high enough to completely suppress radiation diffusion (see text). Benzene fluorescence was used as the reference signal for the measurement reported here.
- R. B. Cundall and A. S. Davies, Trans. Faraday Soc. 62, 1151 (1966).
- C. S. Parmenter and B. L. Ring, J. Chem. Phys. 46, 1998 (1967).
- J. B. Homer and F. P. Lossing, Can. J. Chem. 44, 143 (1966).
- 54. R. Srinivasan, J. Am. Chem. Soc. 89, 4812 (1967).
- 55. H. E. Hunziker, J. Chem. Phys. 50, 1288 (1969)
- 56. E. Jahnke and F. Emde, *Tables of Functions*, 4th Ed., Dover Publications, Inc., New York 1945, p. 246.
- 57. Values of thermal conductivity from Landolt-Börnstein, Zahlenwerte und Funktionen, 6th Ed., Vol. II, Part 5b, Springer-Verlag, Berlin 1968, p. 26.

Received July 16, 1970; revised October 28, 1970

The author is located at the IBM Thomas J. Watson Research Center, Yorktown Heights, New York 10598.